

Interfacial degradation of thermal barrier coatings in isothermal and cyclic oxidation tests

Seol Jeon*, Heesoo Lee*, Youngkue Choi***, Hyun-Gyoo Shin** and Young-Keun Jeong***†

*School of Materials Science and Engineering, Pusan National University, Busan 609-735, Korea

**Material Technology Center, Korea Testing Laboratory, Seoul 152-848, Korea

***Department of Applied Hybrid Materials, Pusan National University, Busan 609-735, Korea

(Received June 26, 2014)

(Revised July 10, 2014)

(Accepted July 18, 2014)

Abstract The degradation mechanisms of thermal barrier coatings (TBCs) were investigated in different thermal fatigue condition in terms of microstructural analyses. The isothermal and cyclic oxidation tests were conducted to atmospheric plasma sprayed-TBCs on NIMONIC 263 substrates. The delamination occurred by the oxide layer formation at the interface, the Ni/Cr-based oxide was formed after Al-based oxide layer grew up to $\sim 10\ \mu\text{m}$ in the isothermal condition. In the cyclic oxidation with dwell time, the failure occurred earlier (500 hr) than in the isothermal oxidation (900 hr) at same temperature. The thickness of Al-based oxide layer of the delaminated specimen in the cyclic condition was $\sim 4\ \mu\text{m}$ and the interfacial cracks were observed. The acoustic emission method revealed that the cracks generated during the cooling step. It was considered that the specimens were prevented from the formation of the Al-based oxide by cooling treatment, and the degradation mode in the cyclic test was dominantly interfacial cracking by the difference of thermal expansion coefficients of the coating layers.

Key words Thermal barrier coating, Thermal fatigue condition, Oxide layer growth, Crack propagation, Degradation mechanism

1. Introduction

Thermal barrier coatings (TBCs) are introduced to metallic materials in gas turbines for power generation with a trend of improving energy efficiency and/or decreasing requirements of cooling system [1-4]. Recently, the required operating temperature of the gas turbines has been increased to $\sim 1,700^\circ\text{C}$ due to the progress of turbine combustion technologies [5, 6].

In the practical condition of the TBCs, the mismatch of thermal expansion coefficient between bond coat (BC) and top coat (TC) layers induces various internal stresses to the interfacial regions. The growth of thermally grown oxide (TGO) layer also applied the stresses to the interfaces, and stress accumulation and relaxation during the thermal cycle can result in crack initiation at the interfaces and coating failures such as delamination and spallation [7, 8].

There are many researches to suppress the early failures and increase the lifetime of the TBCs by improvement of high thermal stability through microstructural

behaviors. Structural design of the coating layers and composition of the TC and BC have been investigated for obtain good properties in high temperature [9-11]. Modeling analyses with a finite element method also is used to expect their degradation behaviors by mathematization of the phenomena in the practical conditions of the TBCs [12, 13].

To evaluate the lifetime of the coating specimens, comprehensive studies should be carried out from a materials design step to an examination of failure mode by a durability test [14]. Therefore, it is important to establish the durability test, which considers the practical condition of the TBCs, and investigate their degradation behaviors according to the thermal stress-inducing methods before lifetime prediction and reliability assessment of the TBCs.

In this study, durability testing methods with different thermal fatigue conditions were designed, and degradation mode and mechanism of TBCs in each test were investigated. An isothermal oxidation test (heating and holding) at chosen temperature and a cyclic oxidation test (heating and cooling) with a dwell time were conducted to atmospheric plasma sprayed-TBCs on superalloy substrates. Failure analyses after the tests were performed on the basis of microstructural observation to

†Corresponding author
Tel: +82-51-510-2483
Fax: +82-51-518-3360
E-mail: nano@pusan.ac.kr

identify their degradation mechanisms.

2. Experimental Procedure

NIMONIC 263, which is an air melted nickel-base alloy with Molybdenum for solid-solution hardening was used for TBC specimen substrates. The substrates were processed as a shape of tensile test specimen, and NiCrAlY based bond coating was deposited on the substrates with thickness of ~150 μm by atmospheric plasma spraying method. 8 wt% Yttria-stabilized zirconia powder [15] was deposited as top coating layer with thickness of ~300 μm on the bond coated specimen.

The specimens were heated in an electric box furnace from room temperature to the chosen temperature - 1,050, 1,100, and 1,200°C (heating as 5°C/min), and

hold 100, 200, 300, 500, 700, and 900 hr in the isothermal oxidation. A schematic picture of testing machine of the cyclic oxidation with dwell time is shown in Fig. 1 [16]. Cooling system was introduced to induce thermal gradient between the coating surface and the substrate. 1,050, 1,100, and 1,150°C were holding temperature in dwell time, and one cycle was composed of heating/cooling as 20 min and dwell time as 1 hr with 100, 200, 300, and 500 cycles. The cooling rate was controlled to maintain the temperature of the coating surface as 80°C. In both tests, the failure of the coating specimens was determined as delamination of the top coating which is identified with naked eyes, and the number of specimens was chosen as nine for each condition.

Failure analysis of the TBC specimens after the thermal fatigue tests was conducted through cross-sectional observation by field-emission scanning electron micros-

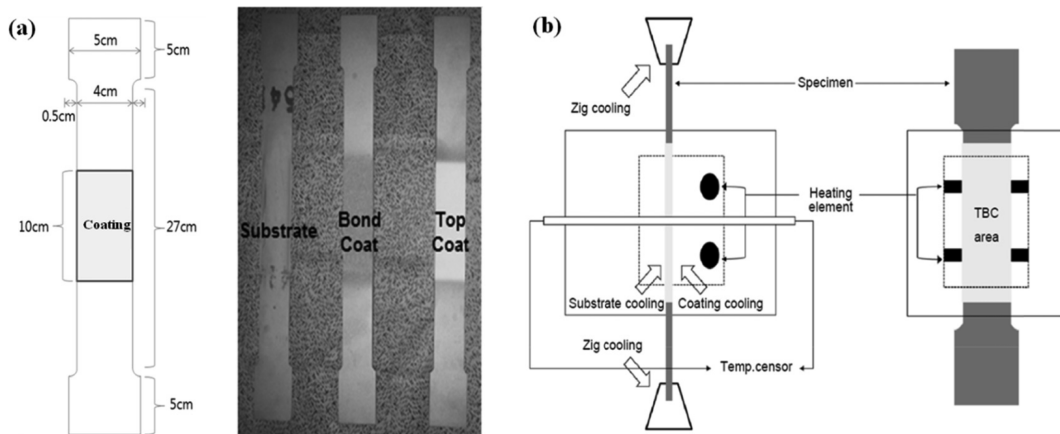


Fig. 1. TBC specimen and testing system: (a) specification of prepared TBC specimens and (b) schematic picture of thermal fatigue testing machine using electric furnace [14].

Table 1
Summary of durability test results according to thermal fatigue conditions

	Temperature (°C)	Failure time (hr)	Failure Mode	
Isothermal (Muffle Furnace) 	1,050	900	Spallation	
	1,100	500		
	1,150	300		
Thermal cycling with dwell time (Cyclic furnace) 	80 - 1,050	300~500 (cycles)	Spallation	
	80 - 1,100	200~300 (cycles)		
	80 - 1,150	100~200 (cycles)		

copy (FE-SEM, S-4700, Hitachi) and energy dispersion spectrum (EDS, EDAX) mapping. Acoustic emission method was introduced in the cyclic oxidation test to identify crack formation and propagation in the TBCs [17]. Acoustic sensors were adhered at both ends of the specimen, and emission of sound from the specimen was measured during the heating, holding, and cooling cycle.

3. Results and Discussion

Results of the durability tests with thermal fatigue condition are summarized in Table 1. The failure time of the TBCs in the isothermal condition was 900, 500, and 300 hr at three different temperature levels - 1,050, 1,100, and 1,150°C, respectively. In the case of the cyclic thermal oxidation with dwell time, the failure time was 300~500, 200~300, and 100~200 hr (cycle) for each

temperature. From these data, it is identified that the cyclic condition with cooling steps was more severe to the TBCs than the holding in same temperature.

Fig. 2 and 3 show cross-sections and EDS mapping of the TBCs after the isothermal oxidation tests, respectively. As shown in Fig. 2(b), (c), and Fig. 3, thermally grown oxides (TGOs) were formed at the BC and TC interfacial regions by reactions between oxygen which infiltrated through the TC layer from air and Al in the BC layer. The thickness of these oxide layers was increased as the exposure time increased. The region in Fig. 3(c) was identified as alumina-based layer generated in the BC layer, and this oxide layer also was caused by the infiltrated oxygen which penetrated the BC layer having many pores [18, 19]. There was Ni and Cr-based oxide region after 500 hr of exposure time (in Fig. 3(c)), and it is expected that this region was also formed by reaction between Ni/Cr in the BC layer and the infiltrated oxygen through the TC layer.

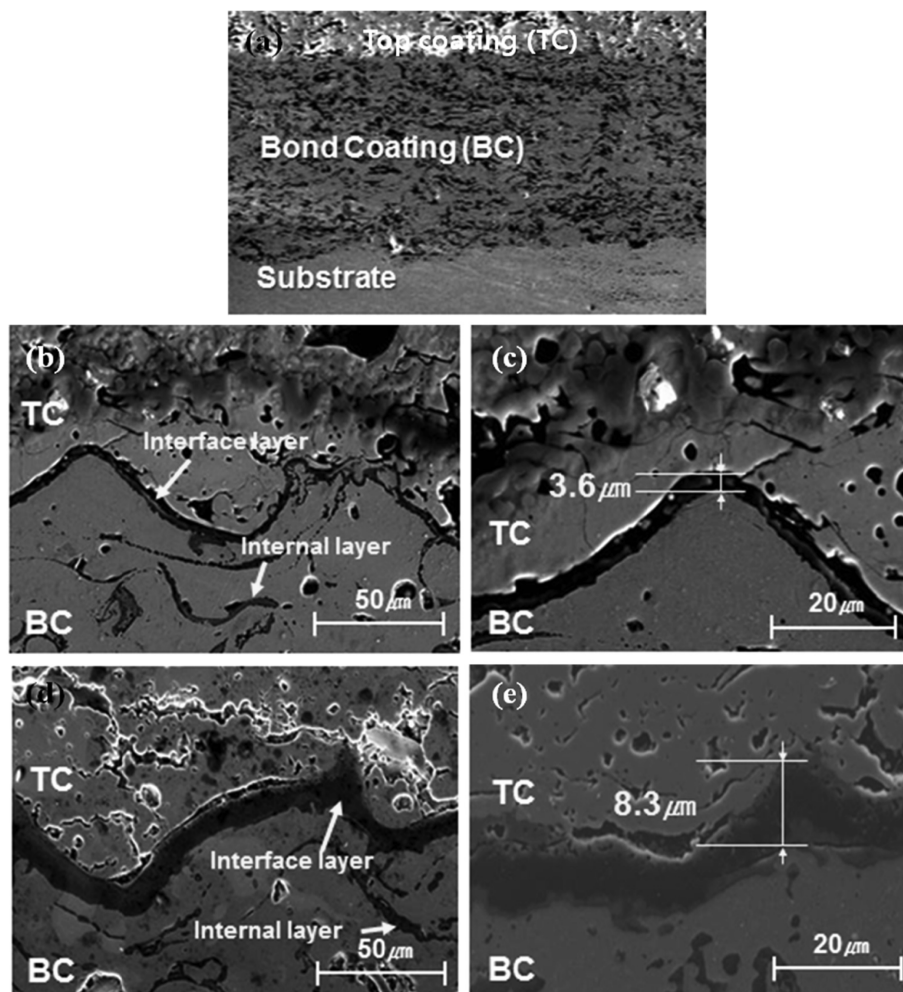


Fig. 2. Cross-sections of thermal barrier coating specimens: (a) as-deposited, exposed at isothermal condition of 1,050°C for (b) and (c) 100 hrs, (d) and (e) 500 hrs.

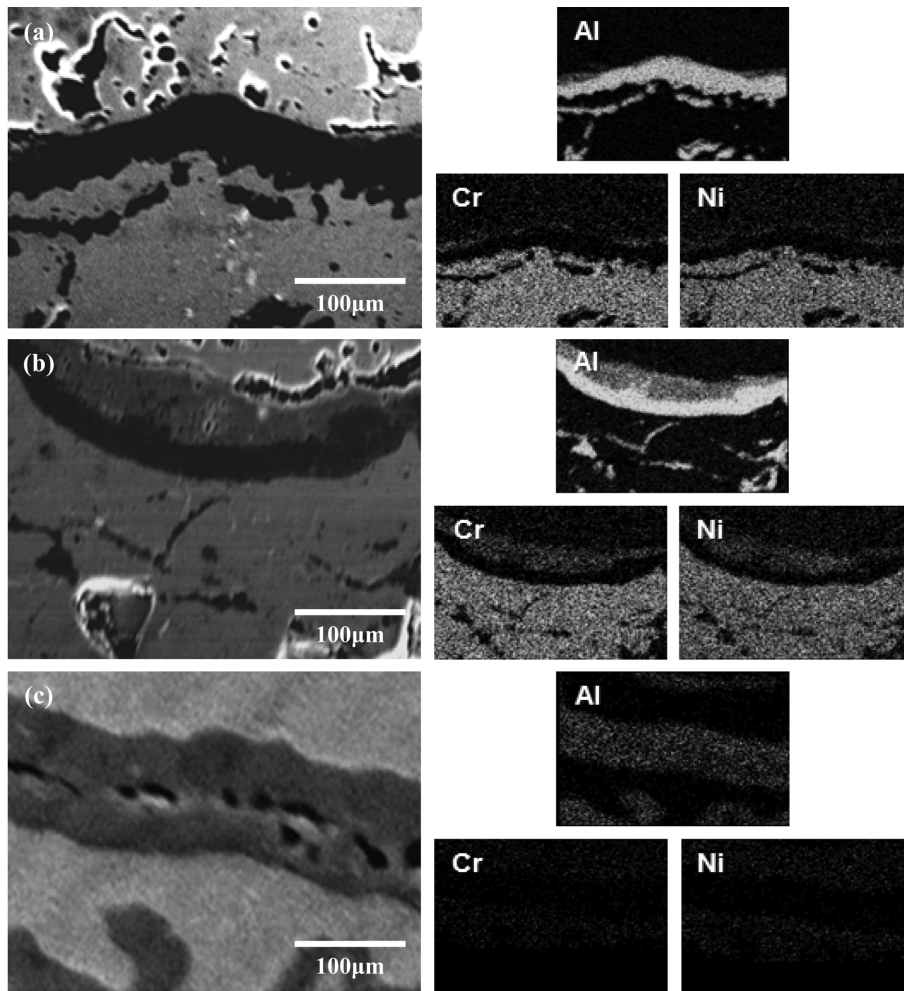


Fig. 3. EDS element mapping of additional layers after 500 hr at isothermal condition of 1,050°C: (a), (b) interfacial, and (c) internal layer.

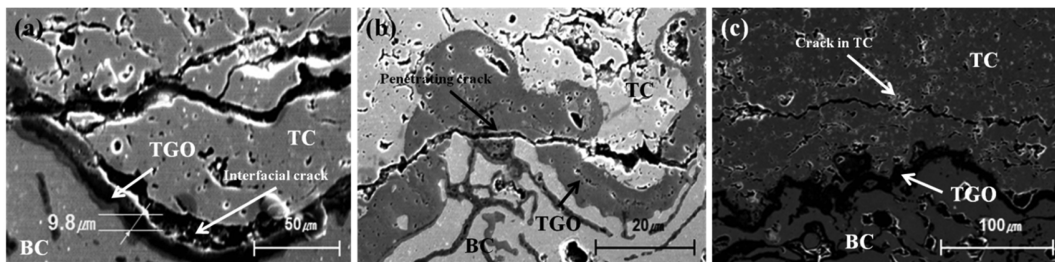


Fig. 4. Microstructure of thermal barrier coating at thermal cycling with dwell time conditions of 1,050°C: (a) crack at TC/BC interface after 100 cycles, (b) penetrating crack through interface after 200 cycles, and (c) crack in TC after 300 cycles.

Cross-sectional images of the TBCs after the cyclic oxidation with dwell time are shown in Fig. 4. It was observed that crack originated from the oxide layer to the TC layer (in Fig. 4(a)) and crack penetrating the Ni/Cr oxide regions (in Fig. 4(b)) were formed during the heating and cooling. The crack closed to the oxide layer and parallel to the TC layer was observed as seen in Fig. 4(c). It is considered that the cyclic oxidation test applies the effects of the holding and the heating/cool-

ing steps to the TBC specimens. Therefore, the crack propagation was similar to that in the isothermal condition, and the cracks were initiated by changes of internal stress due to different of thermal expansion coefficients among the TC, BC layers, and the substrate [20, 21].

Fig. 5 shows changes in thickness of the formed oxide layer and Al contents in TC according to exposure and dwell time. A trend in increasing the thickness of the oxide layer was identified, and the thickness was almost

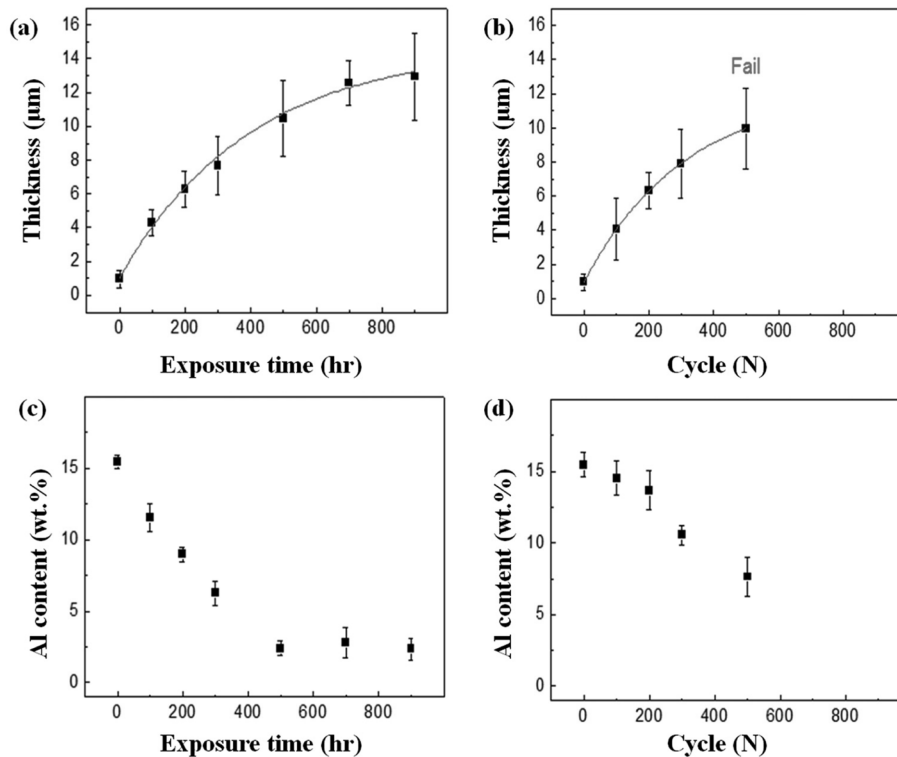


Fig. 5. Changes in thickness of oxide layer and Al contents in BC with exposure time: (a), (c) in isothermal oxidation test and (b), (d) at cyclic oxidation with dwell time at 1,050°C.

constant over 700 hr in the isothermal condition (Fig. 5(a)). It is reasoned that the oxide layer at early stage performed a role as a protective coating layer which suppresses further infiltration of oxygen [22].

As shown in Fig. 5(b), the formed Al-based oxide grew by consume of Al in the BC layer [23-25], after the Al contents continuously were decreased until 500 hr and maintained under 5 at.% over that time. It was reported that Al is thermodynamically unstable and has the highest dissociation pressure among composition elements in the BC layer (Ni, Cr, and Al) Hence, The Al in the BC layer formed the oxide layer with the infiltrated oxygen at first, and the Ni and Cr react with the oxygen and formed the oxide layer after the depletion of Al in the BC layer [26, 27]. Unlike the Al-based oxide layer, the Ni/Cr-based oxide layer has higher brittleness and volume change by oxidation than the Al oxides so that it has a negative effect to lifetime of the TBCs [28].

A similar trend of thickness change in the cyclic condition was identified as seen in Fig. 5(c), and the coating failure was observed at 500 cycles while the Al content was higher than that at 500 hr in the isothermal condition (in Fig. 5(d)). This phenomenon can be explained that the exposure in high temperature was shorter in the cyclic condition than the isothermal oxida-

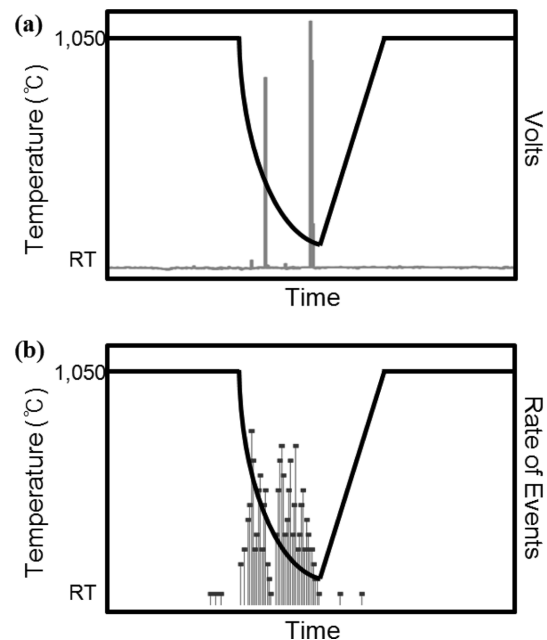


Fig. 6. Results of acoustic emission method according to time and temperature: (a) volt change and (b) emission events in cooling step.

tion, and the cooling step reduced the diffusion and reactivity of Al in the BC layer.

To further understand crack formation and propagation

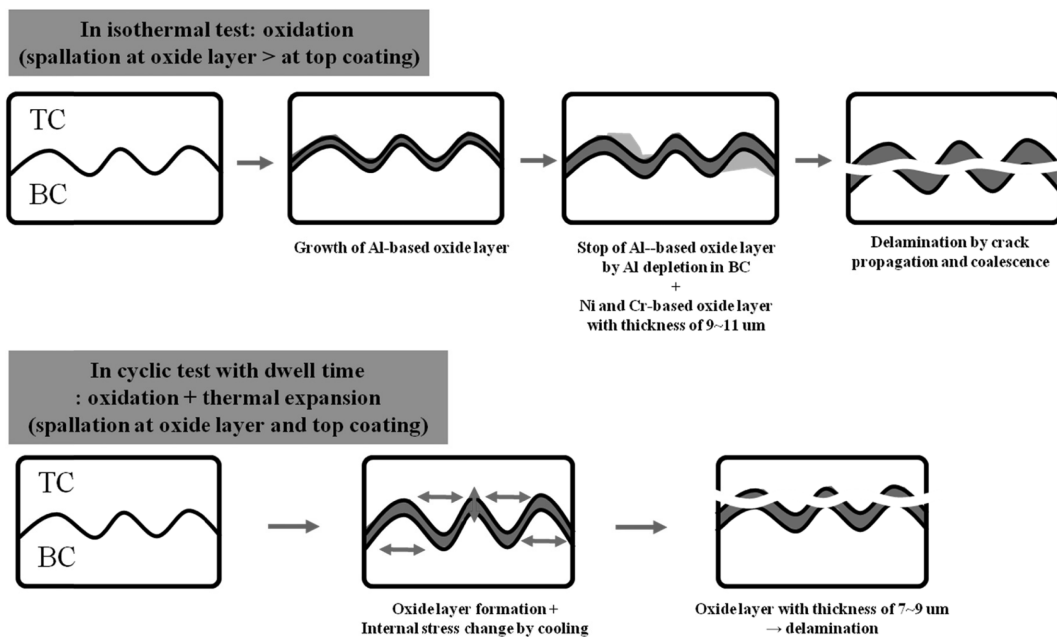


Fig. 7. Schematic picture of degradation and failure mode of TBC specimens by isothermal and cyclic oxidation tests.

behaviors in the TBCs, the Acoustic Emission method was carried out to the specimens in the cyclic condition as shown in Fig. 6. The emissions at regular intervals were identified, and this means that the microcracks were formed and propagated through the changes in internal stresses by volume change with phase transitions in the BC layer around 850 C and the mismatch of thermal expansion coefficients among the coating layers under 300°C [29, 30].

The degradation mode and mechanism of the TBCs by each oxidation condition were described in Fig. 7. In the isothermal condition, the failure of TBCs was caused by the growth of Al-based oxide at the TC-BC interface, and cracking occurred at the oxide layer with and the formation of Ni and Cr-based oxide after the depletion of Al in the BC layer. The Al-based oxide layer was also formed during the heating step in the cyclic oxidation with dwell time. The repeated cooling step generated the thermal expansion mismatch of each coating layer and suppressed the thermal diffusion of Al in BC layer.

4. Conclusion

The degradation mode and mechanism of APS-TBCs were investigated by the durability tests with different oxidation conditions and the failure analyses. The coating failure as delamination in the isothermal condition was caused by the interfacial oxidation at the interfacial

regions, and the Ni/Cr-based oxide layer was formed after Al in the BC layer was depleted by the reaction with infiltrated oxygen. In the case of the cyclic oxidation with dwell time, the thickness of the formed oxide layers was smaller than that in the isothermal condition in same exposure time. The crack formation and propagation in the interfaces were appeared and they caused the earlier failure than in the isothermal oxidation. It is considered that the cooling steps in the cyclic condition prevented the diffusion of Al, and the crack initiation and coalescence at the interface of the oxide layers and the TC layer are main degradation mode by the difference of thermal expansion coefficients during the heating and cooling. Further study for measurement of residual stress changes in the coating layers during thermal oxidation is necessary to improve understanding of degradation behavior and predict the coating failure and lifetime of TBCs.

Acknowledgement

This work was supported by a 2-Year Research Grant of Pusan National University.

References

- [1] J.R. Nicholls, M.J. Deakin and D.S. Rickerby, "A comparison between the erosion behaviour of thermal spray and electron beam physical vapour deposition thermal

- barrier coatings”, *Wear* 233 (1999) 352.
- [2] D. Stöver and C. Funke, “Directions of the development of thermal barrier coatings in energy applications”, *J. Mater. Process. Technol.* 92 (1999) 195.
- [3] W. Beele, G. Marijnissen and A. Van Lieshout, “The evolution of thermal barrier coatings—status and upcoming solutions for today's key issues”, *Surf. Coat. Technol.* 120 (1999) 61.
- [4] B.G. Choi, S.Y. Kim, C.W. Park, J.H. Park, Y.P. Hong and K.B. Shim, “Effect of deposition pressure on the morphology of TiO₂ nanoparticles deposited on Al₂O₃ powders by pulsed laser deposition”, *J. Korean Cryst. Growth Cryst. Technol.* 23 (2013) 167.
- [5] N.P. Padture, M. Gell and E.H. Jordan, “Thermal barrier coatings for gas-turbine engine applications”, *Sci.* 296 (2002) 280.
- [6] H. Echsler, V. Shemet, M. Schütze, L. Singheiser and W.J. Quadackers, “Cracking in and around the thermally grown oxide in thermal barrier coatings: A comparison of isothermal and cyclic oxidation”, *J. Mater. Sci.* 41 (2006) 1047.
- [7] A.G. Evans, D.R. Mumm, J.W. Hutchinson, G.H. Meier and F.S. Pettit, “Mechanisms controlling the durability of thermal barrier coatings”, *Prog. Mater. Sci.* (2001) 505.
- [8] M. Ranjbar-far, J. Absi, G. Mariaux and D.S. Smith, “Crack propagation modeling on the interfaces of thermal barrier coating system with different thickness of the oxide layer and different interface morphologies”, *J. Mat. Design.* 32 (2011) 4961.
- [9] X.Q. Cao, R. Vassen, F. Tietz and D. Stoeber, “New double-ceramic-layer thermal barrier coatings based on zirconia.rare earth composite oxides”, *J. Eur. Ceram. Soc.* 26 (2006) 247.
- [10] W.R. Chen, X. Wu, B.R. Marple, R.S. Lima and P.C. Patnaik, “Pre-oxidation and TGO growth behaviour of an air-plasma-sprayed thermal barrier coating”, *Surf. Coat. Technol.* 202 (2008) 3787.
- [11] A. Afrasiabi, M. Saremi and A. Kobayashi, “A comparative study on hot corrosion resistance of three types of thermal barrier coatings: YSZ, YSZ +Al₂O₃, and YSZ/Al₂O₃”, *Mat. Sci. Eng. A* 478 (2008) 264.
- [12] M. Ranjbar-Far, J. Absi, G. Mariaux and F. Dubois, “Simulation of the effect of material properties and interface roughness on the stress distribution in thermal barrier coatings using finite element method”, *J. Mat. Design.* 31 (2010) 772.
- [13] M. Białas, “Finite element analysis of stress distribution in thermal barrier coatings”, *Surf. Coat. Technol.* 202 (2008) 6002.
- [14] W. Nelson, “Accelerated testing: statistical models, test plans, and data analysis”, 344 (John Wiley & Sons, New York, 2009).
- [15] J.H. Jung, S.J. Yon and J.W. Seok, “Cubic zirconia single crystal growth using shell by skull melting method,” *J. Korean Cryst. Growth Cryst. Technol.* 23 (2013) 124.
- [16] H.G. Shin, Y.K. Choi, S. Jeon, M.S. Jeon and H.S. Lee, “Design of durability and lifetime assessment method under thermomechanical stress for thermal barrier coatings”, *Korean J. Met. Mater.* 52 (2014, In press).
- [17] A.V. Drozdov “Investigation on the microcracking of ceramic materials using the acoustic emission method”, *Strength of Mater.* 46 (2014) 71.
- [18] M. Saremi, A. Afrasiabi and A. Kobayashi, “Bond coat oxidation and hot corrosion behavior of plasma sprayed YSZ coating on Ni superalloy”, *J. Transaction of JWRI* 36 (2007) 41.
- [19] A.C. Fox and T.W. Clyne, “Oxygen transport by gas permeation through the zirconia layer in plasma sprayed thermal barrier coatings”, *Surf. Coat. Technol.* 184 (2004) 311.
- [20] A.G. Evans, D.R. Mumm, J.W. Hutchinson, G.H. Meier and F.S. Pettit, “Mechanisms controlling the durability of thermal barrier coatings”, *Progress in Mater. Sci.* 46 (2001) 505.
- [21] C.H. Hsueh, P.F. Becher, E.R. Fulle, S.A. Lange and W.C. Carter, “Surface-roughness induced residual stresses in thermal barrier coatings: computer simulations”, *In Mater. Sci. Forum* 308 (1999) 442.
- [22] A.M. Limarga, R. Vaßen and D.R. Clarke, “Stress distributions in plasma-sprayed thermal barrier coatings under thermal cycling in a temperature gradient”, *J. Appl. Mech.* 78 (2011) 011003-1.
- [23] J. Toscano, A. Gil, T. Hüttel, E. Wessel, D. Naumenko, L. Singheiser and W.J. Quadackers, “Temperature dependence of phase relationships in different types of MCrAlY-coatings”, *Surf. Coat. Technol.* 202 (2007) 603.
- [24] J. Toscano, R. Vaßen, A. Gil, M. Subanovic, D. Naumenko, L. Singheiser and W.J. Quadackers, “Parameters affecting TGO growth and adherence on MCrAlY-bond coats for TBC’s”, *Surf. Coat. Technol.* 201 (2006) 3906.
- [25] W. Brandl, H.J. Grabke, D. Toma and J. Krüger, “The oxidation behaviour of sprayed MCrAlY coatings”, *Surf. Coat. Technol.* 86 (1996) 41.
- [26] K.A. Khor and Y.W. Gu, “Effects of residual stress on the performance of plasma sprayed functionally graded ZrO₂-NiCoCrAlY coatings”, *Mater. Sci. Eng. A* 277 (2000) 64.
- [27] M. Daroonparvar, M.S. Hussain and M.A.M. Yajid, “The role of formation of continuous thermally grown oxide layer on the nanostructured NiCrAlY bond coat during thermal exposure in air”, *Appl. Surf. Sci.* 261 (2012) 287.
- [28] M. Daroonparvar, M.S. Hussain and M.A.M. Yajid, “The role of formation of continuous thermally grown oxide layer on the nanostructured NiCrAlY bond coat during thermal exposure in air”, *Appl. Surf. Sci.* 261 (2012) 287.
- [29] B. Gudmundsson and B.E. Jacobson, “Structure Formation and Interdiffusion in Vacuum Plasma Sprayed CoNiCrAlY Coatings on IN738LC”, *Mater. Sci. Eng.* 100 (1988) 207.
- [30] M. Schütze, “Protective oxide scales and their breakdown”, D. R. Holmes, Ed., Vol. 1 (John Wiley & Sons, Chichester, 1997).